

Segmentation and Surveying of Cutaneous Hemangiomas *

Sebastian Zambanini¹, Georg Langs^{1,2}, Robert Sablatnig¹

¹ Pattern Recognition and Image Processing Group

Vienna University of Technology, Favoritenstr. 9, A-1040 Vienna, Austria

{zambanis, langs, sab}@prip.tuwien.ac.at

² Institute for Computer Graphics and Vision

Graz University of Technology, Inffeldgasse 16 2.OG, A-8010 Graz, Austria

Abstract

This paper presents an automatic method for the surveying of cutaneous hemangiomas by means of a fully automatic hemangioma segmentation and a ruler visible in the images to be examined. The spatial resolution of the images is determined by computing the maximum Euclidean distance between two marks of the ruler. The segmentation of regions belonging to the hemangioma is accomplished with a pre-segmentation based on a perceptron followed by a postprocessing step where regions with untypical properties are rejected. On a test set of 29 images the segmentation algorithm achieved a false positives rate of 15.5 % and a false negatives rate of 13.1 %.

1 Introduction

Cutaneous hemangiomas are benign tumors made up of newly-formed blood vessels in the skin. Although they are not life-threatening, they may impinge on vital structures and interfere with breathing, vision, eating, or hearing and, especially if occurring in the face, can also cause psychological problems [1].

For the investigation of various methods of treatment it is necessary to determine the area which the hemangioma covers to find out, how much it has increased or decreased since the last examination. In order to make the evaluation of various methods easier, faster, more comfortable and in most cases more precise than a manual segmentation and surveying of the affected skin area, an automated method is highly desirable.

This paper presents an automated method for surveying cutaneous hemangiomas that were photographed along with a ruler to determine the scale of the image. The problem can be divided in two main tasks:

1. Determining the scale of the images by means of the ruler visible in the image.

*This research has been supported by the Austrian Science Fund (FWF) under the grant P17083-N04.

2. Segmentation of the skin area belonging to the hemangioma.

The images used in this project have been kindly provided by the *Department of Dermatology* at the *Vienna General Hospital* which is making a long-range study to compare different methods of treatment for cutaneous hemangiomas. The photos were taken using an analog photo camera and digitalized with a scanner. All images have a resolution of 512x768 pixels and a bit depth of 8 bits per color channel.

In order to increase reliability there are always taken two or more images of the hemangioma, i.e. there are at least two images of a specific hemangioma at a specific date. All images are labeled with a five-digit code to uniquely identify them.

This paper is organized as follows: Section 2 explains in detail the algorithm used for determining the scale of the images. In Section 3 a complete description of the segmentation process used for this project is given, divided into *Preprocessing* (3.1), *Classification* (3.2) and *Post-processing* (3.3). In Section 4 several experiments performed on the data gathered with the algorithm proposed are presented and discussed. A Conclusion is finally given in Section 5.

2 Computing the Scale of the Images

All images of the study show a ruler beside the hemangioma. The ruler has 4 bold lines in 1 cm distance steps. Therefore the task of the algorithm is to compute the Euclidean distance between two lines to get the spatial resolution of the images. The area of the hemangioma is then simply calculated by multiplying the number of hemangioma pixels with the area of one pixel. We neglect the error due to the fact that normally both hemangioma and ruler are not situated on a planar surface parallel to the image plane. The main steps of the algorithm are:

1. Segmenting the ruler: First we have to segment the ruler. Since all rulers are white and differ extremely from the rest of the image, this can simply be done by global thresholding with the *H* and *V* channel of the HSV color model. Sometimes small regions not belonging to the ruler can also remain by this operation, so we take only the largest region in the computed mask.

2. Rotation in horizontal position: In the next step we determine the orientation of the region describing the ruler. For this purpose we calculate the angle between the x-axis and the major axis of the ellipse that has the same second-moments as the region. Once we have this angle, we can rotate the ruler in a horizontal position.

3. Scanlining: For robustness we use three scanlines to determine the number of pixels between two marks. The first scanline is on the midpoint between the top and bottom y-value of the ruler. The two others are 10 pixels above and below, respectively. To determine the scale we take the maximum number of pixels between two marks in all of the three scanlines. With this method we use the part of the ruler which lies most normal to the camera and has the smallest curvature and therefore has to be the most precise measurement. Occasionally it can happen that one or more marks are not recognized in the scanline (e.g. when the ruler has a strong

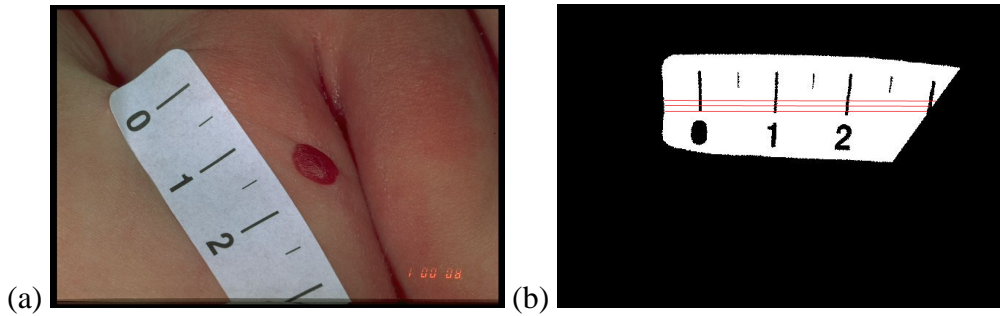


Figure 1: Example for determining the scale of an image

curvature), hence too large distances with more than 200 pixels between two marks are rejected (in all 122 images appropriated for us no greater distance than 155 pixels could be found). If n denotes the number of pixels coming to one cm, the area of one pixel in the image is $(1/n)^2$. An example for determining the scale of an image can be seen in Figure 1: After segmenting and rotating the ruler of Figure 1a, three scanlines are stepped through pixel by pixel to find the maximum distance between two marks (Figure 1b).

3 Segmentation of the Hemangiomas

The task of the segmentation algorithm is to find the regions in an image belonging to the hemangioma. For the special problem of skin lesion segmentation various methods are presented in publications. A thresholding operation is often used for the segmentation of melanomas [2], [3], [12]. Round et al's work on segmentation of skin lesions is basically an application of the split-and-merge algorithm [8]. Schmid and Fischer presented an region-based approach working with two-dimensional histogram analysis and fuzzy c-means clustering technique [10]. Hance et al. [5] compare six different color segmentation algorithms for the special application of finding skin tumor borders (adaptive thresholding, fuzzy c-means, SCT/center split, PCT/median cut, split and merge, multiresolution segmentation) with the conclusion, that the best results can be achieved by adaptive thresholding and the PCT/median cut algorithm or by combining the several methods. Further methods for skin lesion segmentation include radial search [13] and DBSCAN-Clustering [4].

For the segmentation of hemangiomas another approach has to be found. This is mainly caused by the low contrast between skin and hemangioma regions, since hemangiomas mainly appear in bright red [11]. Furthermore, the problem of all color segmentation algorithms is to determine which of the segmented regions are hemangioma regions. Making use of specific a priori knowledge about the general appearance of hemangiomas is difficult because hemangiomas can come in a variety of shapes and sizes (with the exception that very longish regions can be classified as non hemangioma, see Section 3.3.2).

Due to this difficulties we decided to use a classifier for segmenting the images that classifies each pixel in the image as hemangioma or non hemangioma on the basis of its color values.

Although postprocessing is still necessary (see Section 3.3), we get a basic segmentation by this method and can reject regions that are classified erroneously as belonging to the hemangioma later on. For a simple and fast classification we use a single-layer perceptron for that purpose [7]. Multi layer perceptrons were tested but were abandoned since they did not provide significant improvement. Better image acquisition techniques seem to be crucial in order to distinguish between skin colors which are hard to discern even for the medical expert.

In the following our segmentation method is described in detail, divided into a preprocessing step (Section 3.1), a classification step (Section 3.2) and a postprocessing step (Section 3.3).

3.1 Preprocessing

Before the classification step the images have to be preprocessed to improve the accuracy of the perceptron classifier and to reduce computation time. To remove noise a 5x5 median filter is applied on the images. Furthermore, image regions containing no skin are masked out and the images are normalized in such a way that skin has nearly the same color values in all images. These two operations are described below.

3.1.1 Non Skin Masking

A simple test for masking out non skin regions is used after the median filtering to exclude regions that likely are not part of the skin or the hemangioma (e.g. the ruler or dark areas in the background). That step is necessary for a robust determination of the skin's color (see Section 3.1.2) and enhances the speed of the overall segmentation step as well, since not all pixels of the image have to be classified. Our method is based on a heuristic proposed in [5] but substantially simpler. We only check for each pixel, if the red color value is smaller than the green and blue color value. If one of these conditions is complied with, the particular pixel is marked as non skin. This test makes use of the fact that skin has usually a reddish color and therefore shows a greater red portion than green and blue portion. By applying this test on all 122 images we got a almost perfect result for 96 images (classification error less than 1%). The rest shows an average classification error of about 5%. The non skin masking never causes problematic results for the further steps, because the hemangioma and the bigger part of the skin is never masked out.

3.1.2 Normalization with Skin Color

To achieve more accurate classification results a normalization with the skin color has to be done on the images. In other words, we have to determine the color value of the skin in an image and subtract these value from all pixels with the aim of having nearly the same color value of (0,0,0) for skin pixels in all images. For that purpose a 3D histogram of the RGB color channels is created and the maximum RGB value, which has a brightness greater than 120, is taken as skin color (the threshold of 120 was decided to be the most appropriate by empirical tests). This method makes use of the fact that after non skin masking the majority of the remaining pixels in

an image represent skin. Tests have shown that a manual normalization (by choosing three 3x3 windows near the border of the hemangioma and taking the mean color value of all windows as skin color) does not induce better classification results than the histogram normalization which is an indication that this method works accurately.

3.2 Classification of the Hemangiomas

As mentioned before, our segmentation method is based on a perceptron that classifies all pixels in the images by means of their color values. As we see later in Section 3.3, this first segmentation result has to be postprocessed to exclude non hemangioma regions with hemangioma-like color values.

In Section 3.2.1 and 3.2.2 the selection of adequate features for our images is discussed. Section 3.2.3 describes the training phase of the perceptron.

3.2.1 Feature Selection

For classification we have to define a set of features showing a big difference between skin and hemangioma pixels. Possible features for the classification are at first all the three color channels of the significant color spaces RGB, HSV and CIE 1976 L*a*b* [6]. G from RGB, H from HSV and a^* from L*a*b* proved to be usable for our purpose by achieving the best results with a perceptron classification of our images. Further we have created a 4th feature called $abdist$ (see Section 3.2.2). As can be seen in Figure 2, each of these features has a rather big difference between pixels belonging to the hemangioma and pixels belonging to the skin.

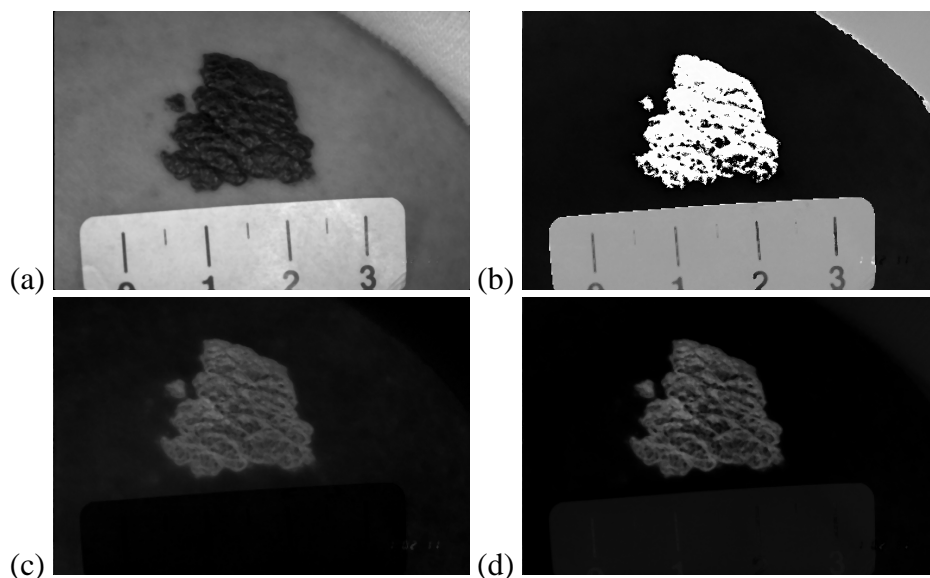


Figure 2: The intensity images of the four features (a) G , (b) H , (c) a and (d) $abdist$ of a particular hemangioma image.

3.2.2 The Feature *abdist*

The feature *abdist* stands for the Euclidean distance between the skin and the hemangioma in the $L^*a^*b^*$ color space without consideration of the luminance L^* and intensification of the a^* component. This feature is adopted from [12]. In this paper the proposed method works on an intensity image describing the Euclidean distance between the skin and the lesion.

If a_s, b_s denotes the a^* and b^* values of the skin (obtained from the normalization step, see 3.1.2) and a_h, b_h that from the hemangioma, *abdist* is computed as follows:

$$abdist = \sqrt{(2a_s - 2a)^2 + (b_s - b)^2} \quad (1)$$

The difference of the a^* channel is multiplied with the factor 2, because the a^* value differs more between hemangioma and skin pixels than the b^* value. At last for contrast enhancement we apply a Gaussian function of the form $G(x) = 1/\sqrt{2\pi\sigma}(1 - \exp(-x^2/2\sigma^2))$ with $\sigma = 0.5$ on the intensity image. This function increases higher values (hemangioma) and decreases lower values (skin) in the intensity image. For an example of *abdist* see Figure 2d.

3.2.3 Training of the Single-Layer Perceptron

To train the perceptron we took a training set of 15 images representing a wide variety of different appearances of hemangiomas. The ground truth was manually determined by ourself by drawing the borders of the hemangiomas in a paint program. All features were brought in the range $[0, 1]$ and normalized with histogram normalization. Best results were achieved with a learning rate $\gamma = 0.0001$ and 50 training cycles. Thereafter no improvement of the classification error was recognized. On the training set the trained perceptron achieved a false positives rate of 30.9% and a false negatives rate of 14.2%.

3.3 Postprocessing

In the postprocessing step several operations are applied to the mask obtained from the classification. To improve the false negatives rate we have to find a way to detect highlights on the hemangioma that were erroneously classified as non hemangioma. Contrariwise we also have to reject regions, which have similar color values to those of the hemangioma but do not belong to it. In the following we describe all operations used to get the final mask.

3.3.1 Hole Closing

For solving the highlights problem mentioned above all holes occurring in the mask are closed. Since hemangiomas with large holes of normal skin could not be found in the 122 images appropriated for us, they seem to be very rare and a possible error resulted from that operation can be neglected. The effect of hole closing can be seen in Figure 3: the highlights detected as non hemangioma by the perceptron (Figure 3a) are added to the mask by hole closing (Figure 3b).

3.3.2 Rejecting Regions

Size-based: First of all regions with a size smaller than 40 pixels are deleted from the mask. In all images no hemangioma region with a size smaller than 60 pixel is contained, therefore this value is proven to be adequate to exclude artifacts.

Position-based: To exclude regions belonging to the five-digit code of the photo, regions having their centroid in a 30x100 frame in the lower right corner of the image are also taken out.

Roundness-based: To detect the erroneously classified regions near the border between skin and dark background areas (that seems to be a special property of the film used in the study) we take advantage of the fact that they mostly stretch over a thin, long line. To discern this regions from hemangioma regions we use *shape descriptors* [9], in particular the *roundness*. Hemangiomas are rather compact and round, so we reject regions with a very small roundness (in this project we used a empirically determined threshold of 0.1).

Color-based: The last criterion we check for each region has to do with his *saturation* and *value* (from the HSV color model). The classifier often chooses by mistake dark and less saturated regions (in comparison to the other regions of the image) to be part of the hemangioma, because they have high values in the *abdist* feature. To exclude these regions we calculate the mean *S* and *V* values of the whole image after non skin masking and compare it with the mean values of the region. That is to say we calculate

$$\frac{Mean(S_{reg})}{Mean(S_{img})} + \frac{Mean(V_{reg})}{Mean(V_{img})} \quad (2)$$

whereas $Mean(S_{reg})$, $Mean(S_{img})$, $Mean(V_{reg})$ and $Mean(V_{img})$ are the mean values of the *S* and *V* values of the image and the region. This computed value is small for regions with a relative low saturation and/or brightness compared to the rest of the image. Therefore, all regions having a lower value calculated with this formula than a specific threshold are deleted from the mask (by testing we found an appropriate threshold of 1.3).

Figure 3 shows the computed hemangioma borders (white) before (Figure 3a) and after (Figure 3b) the postprocessing step of a particular image. The two large, longish regions are rejected because of their low roundness. The false positives rate of this segmentation is decreased from 90.3% to 5.5%, the false negatives rate from 17.7% to 2.2%.

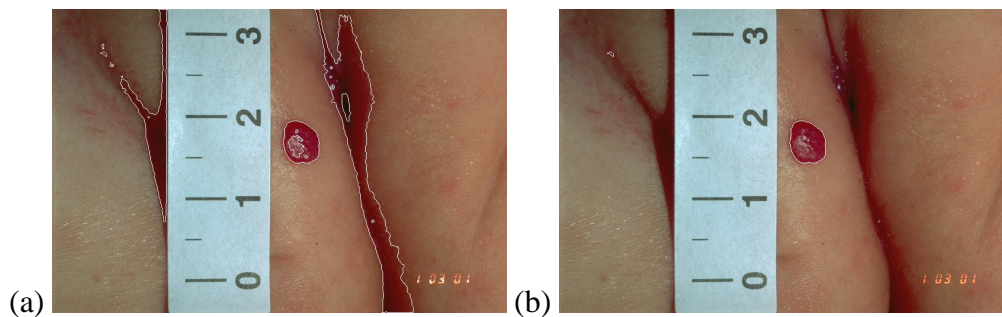


Figure 3: Example of the changes made by the postprocessing step.

4 Experiments

In this section we report experiments with the data gathered and our algorithm applied on it to evaluate the proposed method. Like for the data used in the training phase (Section 3.2.3), the ground truth of the images is annotated manually.

Results on Images and Improvement by Postprocessing: We have tested the segmentation of 29 single images to get an approximation of the overall error rate of the segmentation algorithm proposed. In addition we have tested the effect of the postprocessing step by comparing the false positives and false negatives rate of the same 29 images before and after postprocessing (Table 1). On average by postprocessing we get primarily an improved false positives rate (from **39.0%** to **15.5%**) and also the false negatives rate is decreased (from **17.4%** to **13.1%**). Another important fact is that no image’s error rate is increased significantly by the postprocessing step.

		Before Postprocessing		After Postprocessing				Before Postprocessing		After Postprocessing	
Image	False Pos.	False Neg.	False Pos.	False Neg.	Image	False Pos.	False Neg.	False Pos.	False Neg.		
1	17.7 %	13.3 %	15.9 %	14.3 %	16	9.2 %	40.8 %	0.0 %	5.8 %		
2	0.3 %	12.2 %	0.3 %	10.4 %	17	75.4 %	9.2 %	6.4 %	9.2 %		
3	21.5 %	36.3 %	1.3 %	36.4 %	18	67.9 %	6.7 %	58.9 %	6.7 %		
4	6.3 %	16.1 %	0.8 %	7.9 %	19	29.0 %	14.8 %	24.1 %	14.8 %		
5	41.6 %	27.7 %	9.9 %	27.2 %	20	72.3 %	19.7 %	19.2 %	18.3 %		
6	26.2 %	7.7 %	2.9 %	5.9 %	21	96.2 %	16.1 %	96.2 %	14.2 %		
7	67.6 %	3.2 %	51.4 %	3.2 %	22	26.1 %	8.2 %	6.9 %	8.3 %		
8	1.1 %	8.4 %	0.8 %	2.4 %	23	3.6 %	5.1 %	3.6 %	5.1 %		
9	0.5 %	48.0 %	0.2 %	15.8 %	24	97.2 %	17.2 %	5.2 %	17.2 %		
10	32.3 %	4.0 %	7.1 %	3.9 %	25	52.4 %	5.1 %	43.3 %	5.7 %		
11	3.1 %	12.6 %	2.7 %	10.5 %	26	0.0 %	10.0 %	0.0 %	9.3 %		
12	90.0 %	18.0 %	4.2 %	2.2 %	27	24.0 %	46.9 %	9.4 %	45.7 %		
13	1.3 %	9.1 %	0.6 %	5.3 %	28	49.0 %	6.9 %	1.7 %	4.6 %		
14	89.4 %	46.9 %	11.7 %	46.6 %	29	54.3 %	30.2 %	1.8 %	20.8 %		
15	76.2 %	3.8 %	63.8 %	1.8 %	Average	39.0 %	17.4 %	15.5 %	13.1 %		

Table 1: False positives and false negatives rate of 29 images before and after the postprocessing step.

In Figure 4 we show images of both good and bad segmentation results. Figure 4a-c correspond to images 6, 13, and 28 in Table 1, respectively, and belong to the best segmentation results. Figure 4d-f correspond to images 7, 19 and 21 in Table 1, respectively, and belong to the worst segmentation results.

Comparing Computed Areas of the Same Hemangioma: As mentioned above, all hemangiomas were photographed at least twice, which gave us the possibility to test the precision of the complete algorithm proposed, i.e. the scale computing algorithm combined with the segmentation algorithm. We have computed the areas of two different images displaying the same hemangioma at a specific time of 20 hemangiomas in total. The average error (difference in percent) of all 20 hemangiomas is **0.078 cm²** or rather **11.3%**. This error is mainly caused by the circumstance that two photos of the same hemangioma are never photographed from exactly the same angle.

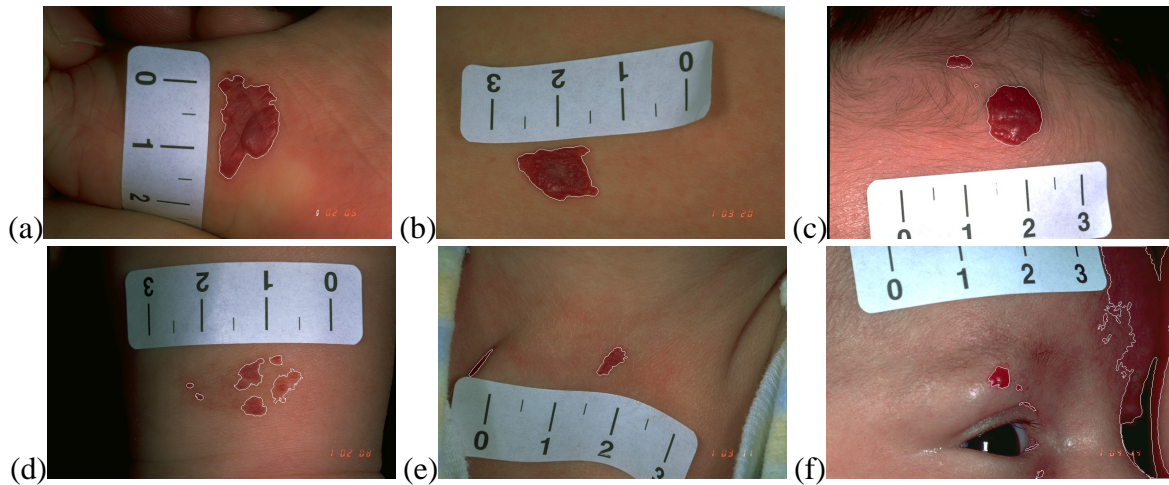


Figure 4: Computed segmentation borders (white) of 6 images with our algorithm.

5 Conclusion

The paper presents a method for the automated measurement of cutaneous hemangiomas in digital images. The algorithm first computes the spatial resolution of an image by determining the euclidean distance between two marks of a ruler contained in the images. Then hemangioma segmentation is accomplished by a single-layer perceptron classification by means of the pixel's color values. In a postprocessing step holes caused by highlights are closed and each segmented region is checked for various properties to exclude falsely classified regions.

Experimental results show that the segmentation is accurate on the majority of images. Bad segmentation results are primarily caused by large regions with hemangioma-like color values that are not rejected in the postprocessing step. For these images a manual definition of a region of interest has to be done to obtain usable segmentation results. Hemangiomas with regressing, slightly reddish parts (e.g. Figure 4d), where it is even difficult for a medical doctor to distinguish between hemangiomas and healthy skin, pose a problem to the algorithm. Here more sophisticated classifiers are expected to improve performance in conjunction with more training data. In general the image acquisition process is crucial to the quality of the results. Inaccuracies in computing the hemangioma area are mainly caused by a less than optimal position of the ruler and hemangioma during acquisition. For an optimal result the perspective distortion has to be taken into account. An improvement of camera position, ruler placement and adequate illumination could contribute considerably to a more precise quantification.

Although the average error of the area calculation (11.3%) seems to be rather high, in most cases the presented automatic method outperforms manual surveying of the images, especially if a region of interest is defined interactively. Thereby clinical trials can be improved by a more consistent evaluation of the effect of therapies.

Acknowledgements: The authors would like to thank Dr. Harald Maier and Prof. Adrian Tanew from the *Vienna General Hospital* for their help and for providing the test images.

References

- [1] Drolet B.A., Esterly N.B. and Frieden N.B., "Hemangiomas in children", *New England Journal of Medicine*, Vol. 341, pp.173-181, July 1999.
- [2] Ganster H., Pinz P., Rohrer R., Wildling E., Binder M. and Kittler H., "Automated melanoma recognition", *IEEE TMI*, Vol. 20, No. 3, pp.233-239, March 2001.
- [3] Green A., Martin N., Pfitzner J., O'Rourke M. and Knight N., "Computer image analysis in the diagnosis of melanoma", *J. of the American Academy of Dermatology*, Vol. 31, No. 6, pp.958-964, December 1994.
- [4] Whenzao Guo and Aslandogan Y.A., "Mining skin lesion images with spatial data mining methods", *Technical Report CSE-2003-19*, Department of Computer Science and Engineering, University of Texas at Arlington, July 2003.
- [5] Hance G.A., Umbaugh S.E., Moss R.H. and Stoecker W.V., "Unsupervised color image segmentation with application to skin tumor borders", *IEEE Engineering in Medicine and Biology*, Vol. 15, No. 1, pp.104-111, January/February 1994.
- [6] Kasson J.M. and Plouffe W., "An Analysis of Selected Computer Interchange Color Spaces", *ACM Transactions on Graphics*, Vol. 11, No. 4, pp.373-405, October 1992.
- [7] Rosenblatt F., "The perceptron: A perceiving and recognizing automaton", *Report 85-460-1*, Project PARA, Cornell Aeronautical Laboratory, Ithaca, New York, January 1957.
- [8] Round A.J., Duller A.W.G. and Fish P.J. "Colour segmentation for lesion classification", *IEEE Proceedings of the Engineering in Medicine and Biology Society*, Vol. 2, pp.582-585, October/November 1997.
- [9] Russ J.C., *The Image Processing Handbook*, CRC Press, Boca Raton, FL, 2nd edition, 1995.
- [10] Schmid P. and Fischer S., "Colour Segmentation for the Analysis of Pigmented Skin Lesions", *Proceedings of the Sixth International Conference on Image Processing and its Applications*, Vol. 2, pp.688-692, July 1997.
- [11] Wirth F.A. and Lowitt M.H., "Diagnosis and Treatment of Cutaneous Vascular Lesions", *American Family Physician*, Vol. 57, No. 4, pp.765-773, February 1998.
- [12] Xu L., Jackowski M., Goshtasby A., Roseman D., Bines S., Yu C., Dhawan A. and Huntley A., "Segmentation of skin cancer images", *Image and Vision Computing*, Vol. 17, No. 1, pp.65-74, January 1999.
- [13] Zhang Z., Stoecker W.V. and Moss R.H., "Border detection on digitized skin tumor images", *IEEE TMI*, Vol. 19, No. 11, pp.1128-1143, November 2000.